J|A|C|S ARTICLES

Published on Web 04/13/2010

Turning on Resonant SERRS Using the Chromophore−Plasmon Coupling Created by Host−Guest Complexation at a Plasmonic Nanoarray

Edward H. Witlicki,[†] Sissel S. Andersen,[‡] Stinne W. Hansen,[‡] Jan O. Jeppesen,[‡] Eric W. Wong,[§] Lasse Jensen,[||] and Amar H. Flood*[,†]

Chemistry Department, Indiana University, 800 East Kirkwood Avenue, Bloomington, Indiana 47405, Department of Physics and Chemistry, University of Southern Denmark, Odense University, Campusvej 55, 5230 Odense M, Denmark, Etamota Corporation, 2672 East Walnut Street, Pasadena, California 91107, and Department of Chemistry, The Pennsylvania State University, 104 Chemistry Building, University Park, Pennsylvania 16802

Received December 1, 2009; E-mail: aflood@indiana.edu

Abstract: An active molecular plasmonics system is demonstrated where a supramolecular chromophore generated in a host−guest binding event *couples* with the localized surface plasmon resonance (LSPR) arising from gold nanodisc gratings. This coupling was achieved by wavelength-matching the chromophore and the LSPR with the laser excitation, thus giving rise to surface-enhanced *resonance* Raman scattering (SERRS). The chromophore is a broad charge-transfer (CT) band centered at 865 nm ($\varepsilon = 3500\ M^{-1}\ cm^{-1}$) generated by the complexation of cyclobis(paraquat-*p*-phenylene) ($CBPQT^{4+}$) and the guest molecule tetrathiafulvalene (TTF). The substrates consist of sub-1-μm gold nanodisc arrays which display dimension-tunable plasmon wavelengths (600−1000 nm). The vibrational spectra of the complex arising from SERRS ($\lambda_{exc} = 785$ nm) were generated by irradiating an array ($\lambda_{LSPR} = 765$ nm) through the solution to give a chromophore-specific signature with the intensities surface enhanced by $\sim 10^5$. Surface adsorption of the empty and complexed $CBPQT^{4+}$ is also implicated in bringing the chromophore into the electric field arising from the surface-localized plasmon. In a titration experiment, the SERRS effect was then used to verify the role of resonance in turning on the spectrum and to accurately quantify the binding between surface-adsorbed $CBPQT^{4+}$ and TTF. The use of a nonpatterned gold substrate as well as a color mismatched complex did not show the enhancement, thus validating that spectral overlap between the chromophore and plasmon resonance is key for resonance surface enhancement. Simulations of the electric fields of the arrays are consistent with interdisc plasmon coupling and the observed enhancement factors. The creation of a responsive plasmonic device upon the addition of the guest molecule and the subsequent coupling of the CT chromophore to the plasmon presents favorable opportunities for applications in molecular sensing and active molecular plasmonics.

Introduction

Active molecular plasmonics is an emerging field[1,2] that creates, studies, and utilizes localized surface plasmon resonances (LSPRs) at molecule−nanostructure interfaces.[3] Motivations for these studies include the potentially high sensitivities[4] arising from surface enhanced Raman scattering[5](SERS) for the sensing[6] of biomolecules,[7] disease markers,[8] and chemical explosives.[9] The LSPRs are also being used directly as local probes for molecular sensing[6,10,11] and information processing.[12] Such studies take advantage of the intense electric fields associated with the near-field LSPRs that can be driven by light excitation and which extend into the space surrounding the nanostructure by a few nanometers.[13] The majority of recent advances in SERS and plasmonics have been facilitated by the controllable fabrication of nanomaterials with tunable shapes and sizes and, therefore, optical properties. In light of these developments, the timing is right to begin interfacing these

[†] Indiana University.
[‡] Odense University.
[§] Etamota Corporation.
[||] The Pennsylvania State University.

(1) (a) Van Duyne, R. P.; Hulteen, J. C.; Treichel, D. A. *J. Chem. Phys.* **1993**, *3*, 2101–2115. (b) Kometani, N.; Tsubonishi, M.; Fujita, T.; Asami, K.; Yonezawa, Y. *Langmuir* **2001**, *17*, 578–580. (c) Prodan, E.; Nordlander, P. *Nano Lett.* **2003**, *3*, 543–547. (d) Wang, Z.; Chumanov, G. *Adv. Mater.* **2003**, *15*, 1285–1289. (e) Badolato, A.; Hennessy, K.; Atatüre, M.; Dreiser, J.; Hu, E.; Petroff, P.; Imamoğlu, A. *Science* **2005**, *308*, 1158–1161. (f) Haes, A. J.; Zhao, J.; Zou, S.; Own, C. S.; Marks, L. D.; Schatz, G. C.; Van Duyne, R. P. *J. Phys. Chem. B* **2005**, *109*, 11158–11162. (g) Ambjörnsson, T.; Mukhopadhyay, G.; Apell, S. P.; Käll, M. *Phys. Rev. B* **2006**, *73*, 085412. (h) Sugawara, Y.; Kelf, T. A.; Baumberg, J. J.; Adbelsalam, M. E.; Bartlett, P. N. *Phys. Rev. Lett.* **2006**, *97*, 1–4. (i) Kelley, A. M. *Nano Lett.* **2007**, *7*, 3235–3240. (j) Uwada, T.; Toyota, R.; Masuhara, H.; Asashi, T. *J. Phys. Chem. C* **2007**, *111*, 1549–1552. (k) Wang, H.; Kundu, J.; Halas, N. *Angew. Chem., Int. Ed.* **2007**, *46*, 1–6. (l) Hao, F.; Nordlander, P.; Burnett, M. T.; Maier, S. A. *Phys. Rev. B* **2007**, *76*, 245417-1–245417-6. (m) Zhao, J.; Jensen, L.; Sung, J.; Zou, S.; Schatz, G. C.; Van Duyne, R. P. *J. Am. Chem. Soc.* **2007**, *129*, 7647–7657. (n) Mahmoud, M. A.; El-Sayed, M. A. *J. Phys. Chem. C* **2008**, *112*, 14618–14625. (o) Nordlander, P. *ACS Nano* **2009**, *3*, 488–492. Juluri, B. K.; Lu, M.; Zheng, Y. B.; Huang, T. J.; Jensen, L. *J. Phys. Chem. C* **2009**, *113*, 18499–18503. (p) Hao, F.; Nordlander, P.; Sonnefraud, Y.; Dorpe, P. V.; Maier, S. A. *ACS Nano* **2009**, *3*, 643–652.

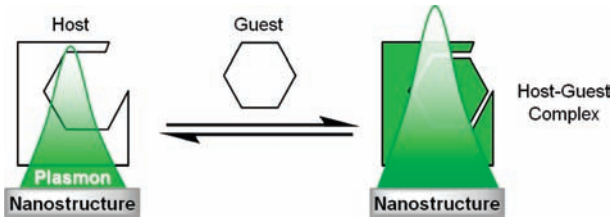

Figure 1. When a host binds a guest to generate a colored host−guest complex within the proximity of a plasmonically active nanostructure, it becomes possible for the supramolecular chromophore and plasmon to couple together, thereby enhancing the local electric field.

tunable plasmonic structures with designer molecules to achieve integrated systems that can display greater functionality. One of the simplest demonstrations of this approach is to show how the binding of a molecular host with a guest can generate a colored chromophore that couples to the LSPR (Figure 1) of a plasmonically active nanostructure leading to spectral, resonance, and surface enhancements.

One elementary way to achieve active molecular plasmonics[1,14] is to use functional molecules with colored chromophores that have absorption maxima coincident with the wavelengths of LSPRs. A few early precedents fulfill some or all of these criteria. Spectroscopy of rhodamine-6G using surface-enhanced resonance Raman scattering (SERRS)[15] achieves wavelength-matching between both chromophore and plasmon. Imaging and spectroscopy of conjugates between gold nanoparticles and cytochrome *c*[16] suggest plasmon resonance energy transfer between nanoparticles and the adsorbed molecules. J-Aggregates of thiacyanines show evidence for exciton−plasmon couplings.[17] Photochromic spiropyrans[18] and redox-stimulated polyaniline[19] alter the position of plasmon frequencies. Considering the functionality that can be introduced with supramolecular systems and the applications in molecular sensing, past studies have combined SERS[20] with traditional hosts such as crown ethers,[21] calixarenes,[22] cyclodextrins,[23] and resorcinarenes[13d] to quantify and detect analyte binding. These quantitative studies take advantage of the changes in vibrational signatures corresponding to the structural changes commensurate with binding and usually "turn on" the detection of an analyte by the mechanism of preconcentration. Recently, stimuli-responsive systems in the form of surface-bound bistable rotaxanes[12] or a pH-dependent

(2) We broadly define "active molecular plasmonics" as and when the surface plasmons and the electromagnetic properties of the molecule, (e.g., dielectric constant, polarizability, dipole, hyperpolarizability) interact with each other at sufficient strengths to allow one to manipulate the other's properties.

(3) (a) Lu, T.; Cotton, T. M.; Hurst, J. K.; Thompson, D. H. P. *J. Phys. Chem.* **1988**, *92*, 6978–6985. (b) Tang, X.; Schneider, T.; Buttry, D. A. *Langmuir* **1994**, *10*, 2235–2240. (c) Kreisig, S.; Tarazona, A.; Koglin, E. *Electrochim. Acta* **1997**, *42*, 3335–3344. (d) Abdelsalam, M. E.; Bartlett, P. N.; Baumberg, J. J.; Cintra, S.; Kelf, T. A.; Russell, A. E. *Electrochem. Commun.* **2005**, *7*, 740–744. (e) Baumberg, J. J.; Kelf, T. A.; Sugawara, Y.; Cintra, S.; Abdelsalam, M. E.; Bartlett, P. N.; Russell, A. E. *Nano Lett.* **2005**, *5*, 2262–2267. (f) Ozbay, E. *Science* **2006**, *311*, 189–193. (g) Mažeikienė, R.; Niaura, G.; Malinauskas, A. *Electrochim. Acta* **2008**, *53*, 7736–7743. (h) Mahajan, S.; Cole, R. M.; Soares, B. F.; Pelfrey, S. H.; Russell, A. E.; Baumberg, J. J.; Bartlett, P. N. *J. Phys. Chem. C* **2009**, *113*, 9284–9289. (i) Feng, J.-J.; Gernert, U.; Sezer, M.; Kuhlmann, U.; Murgida, D. H.; David, C.; Richter, M.; Knorr, A.; Hildebrandt, P.; Weidinger, I. M. *Nano Lett.* **2009**, *9*, 298–303. (j) Morton, S. M.; Jensen, L. *J. Am. Chem. Soc.* **2009**, *131*, 4090–4098.

(4) Tolaieb, B.; Constantino, C. J. L.; Aroca, R. F. *Analyst* **2004**, *129*, 337–341.

(5) (a) Fleischman, M.; Hendra, P. J.; McQuillan, A. J. *Chem. Phys. Lett.* **1974**, *26*, 163–166. (b) Jeanmaire, D. L.; Van Duyne, R. P. *J. Electroanal. Chem.* **1977**, *84*, 1–20. (c) Albrecht, M. G.; Creighton, J. A. *J. Am. Chem. Soc.* **1977**, *99*, 5215–5217. Garrell, R. L. *Anal. Chem.* **1989**, *61*, 401–411. (d) Freeman, R. G.; Grabar, K. C.; Allison, K. J.; Bright, R. M.; Davis, J. A.; Guthrie, A. P.; Hommer, M. B.; Jackson, M. A.; Smith, P. C.; Walter, D. G.; Natan, M. J. *Science* **1995**, *267*, 1629–1632. (e) Grabar, K. C.; Freeman, R. G.; Hommer, M. B.; Natan, M. *J. Anal. Chem.* **1995**, *67*, 735–743. (f) Grabar, K. C.; Smith, P. C.; Musick, M. D.; Davis, J. A.; Walter, D. G.; Jackson, M. A.; Guthrie, A. P.; Natan, M. J. *J. Am. Chem. Soc.* **1996**, *118*, 1148–1153. (g) Kneipp, K.; Kneipp, H.; Itzkan, I.; Dasari, R. R.; Feld, M. S. *J. Phys.: Condens. Matter.* **2002**, *14*, 597–624. (h) Zangmeister, C. D.; Robey, S. W.; van Zee, R. D.; Yao, Y.; Tour, J. M. *J. Phys. Chem.* **2004**, *108*, 16187–16193. (i) Haynes, C.; McFarland, A. D.; Van Duyne, R. P. *Anal. Chem.* **2005**, *77*, 339–346. (j) Dieringer, J. A.; McFarland, A. D.; Shah, N. C.; Stuart, D. A.; Whitney, A. V.; Yonzon, C. R.; Young, M. A.; Zhang, X.; Van Duyne, R. P. *Faraday Discuss.* **2006**, *132*, 9–26. (k) Aroca, R. *Surface-Enhanced Vibrational Spectroscopy*; Wiley: Hoboken, NJ, 2006. (l) Willets, K. A.; Van Duyne, R. P. *Annu. Rev. Phys. Chem.* **2007**, *58*, 267–97.

(6) Golightly, R. S.; Doering, W. E.; Natan, M. J. *ACS Nano* **2009**, *10*, 2859–2869.

(7) (a) Dick, L. A.; Haes, A. J.; Van Duyne, R. P. *J. Phys. Chem. B* **2000**, *104*, 11752–11762. (b) Tian, Z.-Q.; Ren, B.; Wu, D.-Y. *J. Phys. Chem. B* **2002**, *106*, 9463–9483. (c) Grubisha, D. S.; Lipert, R. J.; Park, H. Y.; Driskell, J.; Porter, M. D. *Anal. Chem.* **2003**, *75*, 5936–5943. (d) Fromm, D. P.; Sundaramurthy, A.; Schuck, P. J.; Kino, G.; Moerner, W. E. *Nano Lett.* **2004**, *4*, 957–961. (e) Stuart, D. A.; Yonzon, C. R.; Zhang, X.; Lyandres, O.; Shah, N. C.; Glucksberg, M. R.; Walsh, J. T.; Van Duyne, R. P. *Anal. Chem.* **2005**, *77*, 4013–4019. (f) Wang, H.; Levin, C. S.; Halas, N. J. *J. Am. Chem. Soc.* **2005**, *127*, 14992–14993. (g) Su, X.; Zhang, J.; Sun, L.; Koo, T.-W.; Chan, S.; Sundararajan, M.; Yamakawa, M.; Berlin, A. A. *Nano Lett.* **2005**, *5*, 49–54. (h) Braun, G.; Lee, S. J.; Dante, M.; Nguyen, T.-Q.; Moskovits, M.; Reich, N. *J. Am. Chem. Soc.* **2007**, *129*, 6378–6379. (i) Lytton-Jean, A. K. R.; Han, M. S.; Mirkin, C. A. *Anal. Chem.* **2007**, *79*, 6037–6041. (j) Tognalli, N. G.; Scodellar, P.; Flexer, V.; Szamocki, R.; Ricci, A.; Tagliazucchi, M.; Calvo, E. J.; Fainstein, A. *Phys. Chem. Chem. Phys.* **2009**, *11*, 7412–7423.

(8) (a) Grabbe, E. S.; Buck, R. P. *J. Electroanal. Chem.* **1991**, *308*, 227–237. (b) Mosier-Boss, P. A.; Lieberman, S. H. *Appl. Spectrosc.* **2003**, *57*, 1129–1137. (c) Jarvis, R. M.; Goodacre, R. *Anal. Chem.* **2004**, *76*, 40–47. (d) Bell, S. E. J.; Mackle, J. N.; Sirimuthu, N. M. S. *Analyst* **2005**, *130*, 545–549. (e) Rosi, N. L.; Mirkin, C. A. *Chem. Rev.* **2005**, 1547–1562. (f) Xu, S.; Ji, X.; Xu, W.; Zhao, B.; Dou, X.; Bai, Y.; Ozaki, Y. *J. Biomed. Opt.* **2005**, *10*, 031112. (g) Pavel, I.; McCarney, E.; Elkhaled, A.; Morrill, A.; Plaxco, K.; Moskovits, M. *J. Phys. Chem. C* **2008**, *112*, 4880–4883.

(9) (a) Pemberton, J. E.; Buck, R. P. *Anal. Chem.* **1981**, *53*, 2263–2267. (b) Syliva, J. M.; Janni, J. A.; Klein, J. D.; Spencer, K. M. *Anal. Chem.* **2000**, *23*, 5834–5840. (c) Baker, G. A.; Moore, D. S. *Anal. Bioanal. Chem.* **2005**, *8*, 1751–1770.

(10) (a) Cao, Y. W. C.; Jin, R.; Mirkin, C. A. *Science* **2002**, *297*, 1536–1540. (b) Piorek, B. D.; Lee, S. J.; Santiago, J. G.; Moskovits, M.; Banerjee, S.; Meinhart, C. D. *Proc. Natl. Acad. Sci. U.S.A.* **2007**, *48*, 18898–18901.

(11) Larsson, E. M.; Langhammer, C.; Zoric, I.; Kasemo, B. *Science* **2009**, *326*, 1091–1094.

(12) (a) Wei, A. *Chem. Commun.* **2006**, *15*, 1581–1591. (b) Zheng, Y. B.; Yang, Y.-W.; Jensen, L.; Fang, L.; Juluri, B. K.; Flood, A. H.; Weiss, P. S.; Stoddart, J. F.; Huang, T. J. *Nano Lett.* **2009**, *9*, 819–825.

(13) (a) Gersten, J.; Nitzan, A. *J. Chem. Phys.* **1980**, *7*, 3023–3037. (b) Campion, A.; Kambhampati, P. *Chem. Soc. Rev.* **1998**, *4*, 241–250. (c) McCreery, R. L. *Raman Spectroscopy for Chemical Analysis*; Wiley: New York, 2000. (d) Wei, A.; Kim, B.; Sadtler, B.; Tripp, S. L. *ChemPhysChem* **2001**, *2*, 743–745. (e) Otto, A. *J. Raman Spectrosc.* **2002**, *8*, 593–598. (f) Jiang, J.; Bosnick, K.; Maillard, M.; Brus, L. *J. Phys. Chem. B* **2003**, *37*, 9964–9972.

(14) Haes, A. J.; Haynes, C. L.; McFarland, A. D.; Schatz, G. C.; Van Duyne, R. R.; Zou, S. L. *MRS Bull.* **2005**, *30*, 368–375.

(15) (a) Nie, S. M.; Emory, S. R. *Science* **1997**, *275*, 1102–1106. (b) Doering, W. E.; Nie, S. *J. Phys. Chem. B* **2002**, *106*, 311–317. (c) Haes, A. J.; Zou, S.; Schatz, G. C.; Van Duyne, R. P. *J. Am. Chem. Soc.* **2006**, *128*, 10905–10914.

(16) Liu, G. L.; Long, Y. T.; Choi, Y.; Kang, T.; Lee, L. P. *Nat. Methods* **2007**, *4*, 1015–1017.

(17) Wiederrecht, G. P.; Wurtz, G. A.; Hranisavljevic, J. *Nano Lett.* **2004**, *4*, 2121–2125.

(18) Pala, R. A.; Shimizu, K. T.; Melosh, N. A.; Brongersma, M. L. *Nano Lett.* **2008**, *8*, 1506–1510.

(19) Leroux, Y.; Lacroix, J. C.; Fave, C.; Trippe, G.; Felidj, N.; Aubard, J.; Hohenau, A.; Krenn, J. R. *ACS Nano* **2008**, *2*, 728–732.

block copolymer[24] have been used to reversibly switch either the position of the LSPR frequencies or the SERS response, respectively. These examples broaden the complexity of plasmonics systems to include the properties that can be brought into play by synthetic molecules.[25] The present work represents a new principle for active molecular plasmonics where the chromophore generated upon the formation of a host−guest complex, rather than adding[23b] or modifying a resonant species,[20b] can couple to the LSPR to turn on a SERRS response and thus the intensity of the resulting spectrum.

Herein, we describe such an integrated active molecular plasmonics system (Figure 1). The plasmons arising from dimension-tunable gold nanodisc arrays were investigated individually, and the array with an LSPR that is wavelength-matched for both laser excitation (785 nm) and the charge-transfer (CT) chromophore (865 nm) of the complex formed between tetrathiafulvalene (TTF) and cyclobis(paraquat-*p*-phenylene) ($CBPQT^{4+}$) was utilized. Quantitative titration of TTF into a solution of $CBPQT^{4+}$ creates the green colored complex $TTF\subset CBPQT^{4+}$. When this solution is interfaced with the plasmonic array, the adsorption of the complex at the surface allows chromophore−plasmon coupling to occur as determined by an analysis of the resonance-based SERRS spectra.

Plasmonics Design. The substrates developed for the present study are based on previous research showing how periodic lattices of metal particles can be used to generate strong plasmon resonances that localize between the particles with high SERS enhancements.[26] Herein, two-dimensional gratings[27] are used that are composed of silicon oxide patterned and etched into lattices of hexagonally close-packed nanodiscs which are then overcoated with a continuous layer of gold to render them plasmonically active. The process uses UV lithography which is amenable to batch processing instead of electron beam lithography,[28] which is slow and costly, or self-assembly,[29,30] which has not been shown to be amenable to precise wafer-scale processing. As with other substrate designs based on periodic lattices or gratings,[3,28,31] the nanodisc arrays have plasmons that can be conveniently tuned by choosing the lattice dimension parameters. The dimension tunability of each of these structures is confirmed using reflectance absorption UV−vis−NIR spectroscopy with the unpatterned regions serving as useful control surfaces.

Scheme 1. Representations of the Complexation between Cyclobis(paraquat-*p*-phenylene) ($CBPQT^{4+}$) and (a) Tetrathiafulvalene (TTF) and (b) Control Molecule 1,5-Dimethoxynaphthalene (DNP)

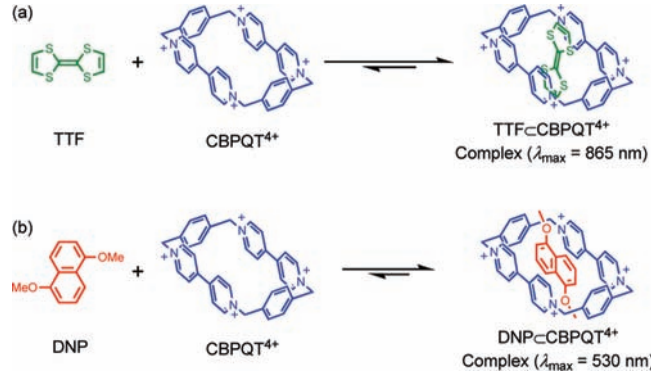

Supramolecular Experimental Design. The supramolecular element of the system (Scheme 1a) utilizes the electron-donating TTF[32] molecule as a guest for the electron accepting macrocyclic host[33] $CBPQT^{4+}$ to form a well-known[34] donor−acceptor complex ($\Delta G_a = -5.6 \pm 0.3$ kcal mol^{-1}, MeCN, 298 K) with a CT transition centered at $\lambda_{max} = 865$ nm ($\varepsilon = 3500$ M^{-1} cm^{-1}). The resonance Raman scattering spectra of the resulting solution-phase complex, $TTF\subset CBPQT^{4+}$ (Scheme 1a), its binding and chromophore generation, and a density-functional theory (DFT) assignment of the vibrational bands have been

(20) (a) McGlashen, M. L.; Davis, K. L.; Morris, M. D. *Anal. Chem.* **1990**, *62*, 846–849. (b) Carron, K.; Mullen, K.; Lanouette, M.; Angersbach, H. *Appl. Spectrosc.* **1991**, *45*, 420–423. (c) Carron, K.; Peitersen, L.; Lewis, M. *Environ. Sci. Technol.* **1992**, *26*, 1950–1954. (d) Schierbaum, K. D.; Weiss, T.; van Velzen, E. U. T.; Engbersen, J. F. J.; Reinhoudt, D. N.; Göpel, W. *Science* **1994**, *265*, 1413–1415. (e) Crane, L. G.; Wang, D.; Sears, L. M.; Heynes, J. B.; Carron, K. *Anal. Chem.* **1995**, *67*, 360–364. (f) Teiten, B.; Burneau, A. *J. Raman Spectrosc.* **1997**, *28*, 879–884. (g) Kanayama, N.; Kanbara, T.; Kitano, H. *J. Phys. Chem. B* **2000**, *104*, 271–278. (h) Uibel, R. H.; Harris, J. M. *Appl. Spectrosc.* **2000**, *54*, 1868–1875. (i) Mosier-Boss, P. A.; Lieberman, S. H. *Appl. Spectrosc.* **2003**, *57*, 1129–1137. (j) Kanayama, N.; Kitano, H. *Langmuir* **2000**, *16*, 577–583. (k) Alaverdian, I. S.; Feofanov, A. V.; Gromov, S. P.; Vedernikov, A. I.; Lobova, N. A.; Alfimov, M. V. *J. Phys. Chem. A* **2003**, *107*, 9542–9546. (l) Alaverdyan, Y. S.; Feofanov, A. V.; Gromov, S. P.; Vedernikov, A. I.; Lobova, N. A.; Alfimov, M. V. *Opt. Spectrosc.* **2004**, *97*, 560–566. (m) Leyton, P.; Sanchez-Cortes, S.; Garcia-Ramos, J. V.; Domingo, C.; Campos-Vallette, M.; Saitz, C.; Clavijo, R. E. *J. Phys. Chem. B* **2004**, *108*, 17484–17490. (n) Guerrini, L.; Garcia-Ramos, J. V.; Domingo, C.; Sanchez-Cortes, S. *J. Phys. Chem. C* **2008**, *112*, 7527–7530. (o) Guerrini, L.; Garcia-Ramos, J. V.; Domingo, C.; Sanchez-Cortes, S. *Phys. Chem. Chem. Phys.* **2009**, *11*, 1787–1793.
(21) Heyns, J. B.; Sears, L. M.; Corcoran, R. C.; Carron, K. T. *Anal. Chem.* **1994**, *66*, 1572–1574.
(22) (a) Hill, W.; Wehling, B.; Gibbs, C. G.; Gutsche, C. D.; Klockow, D. *Anal. Chem.* **1995**, *67*, 3187–3192. (b) Marenco, C.; Stirling, C. J. M.; Yarwood, J. *J. Raman Spectrosc.* **2001**, *32*, 183–194. (c) Mosier-Boss, P. A. *Appl. Spectrosc.* **2006**, *60*, 1148–1156.
(23) (a) Maeda, Y.; Kitano, H. *J. Phys. Chem.* **1995**, *99*, 487–488. (b) Hill, W.; Fallourd, V.; Klockow, D. *J. Phys. Chem. B* **1999**, *103*, 4707–4713. (c) McNally, A.; Forster, R. J.; Keyes, T. E. *Phys. Chem. Chem. Phys.* **2009**, *11*, 848–856.
(24) Qian, X.; Li, J.; Nie, S. *J. Am. Chem. Soc.* **2009**, *131*, 7540–7541.
(25) Flood, A. H.; Ramirez, R. J. A.; Deng, W.-Q.; Muller, R. P.; Goddard, W. A.; Stoddart, J. F. *Aust. J. Chem.* **2004**, *57*, 301–322.
(26) (a) Kahl, M.; Voges, E.; Kostrewa, S.; Viets, C.; Hill, W. *Sens. Actuators, B* **1998**, *51*, 285–291. (b) Kahl, M.; Voges, E. *Phys. Rev. B* **2000**, *61*, 14078–14088. (c) Haynes, C. L.; McFarland, A. D.; Zhao, L.; Van Duyne, R. P.; Schatz, G. C.; Gunnarsson, L.; Prikulis, J.; Kasemo, B.; Kall, M. *J. Phys. Chem. B* **2003**, *107*, 7337–7342. (d) Tao, A.; Kim, F.; Hess, C.; Goldberger, J.; He, R.; Sun, Y.; Xia, Y.; Yang, P. *Nano Lett.* **2003**, *3*, 1229–1233. (e) Genov, D. A.; Sarychev, A. K.; Shalaev, V. M.; Wei, A. *Nano Lett.* **2004**, *4*, 153–158. (f) Hicks, E. M.; Zhang, X.; Zou, S.; Lyandres, O.; Spears, K. G. S.; Schatz, G. C.; Van Duyne, R. P. *J. Phys. Chem. B* **2005**, *109*, 22351–22358. (g) Lee, S. J.; Guan, Z.; Xu, H.; Moskovits, M. *J. Phys. Chem. C* **2007**, *111*, 17985–17988. (h) Lin, T.-H.; Linn, N. C.; Tarajano, L.; Jiang, B.; Jiang, P. *J. Phys. Chem. C* **2009**, *113*, 1367–1372. (i) Liu, X.; Sun, C.-H.; Linn, N. C.; Jiang, B.; Jiang, P. *J. Phys. Chem. C* **2009**, *113*, 14804–14811.
(27) (a) Raether, H. *Surface Plasmons on Smooth and Rough Surfaces and on Gratings*; Springer-Verlag: Berlin, 1988 (b) Loewen, E. G., Popov, E., Ed. *Diffraction Gratings and Applications*; Marcel-Dekker: New York, 1997.
(28) (a) Lamprecht, B.; Schider, G.; Lechner, R. T.; Ditlbacher, H.; Krenn, J. R.; Leitner, A.; Ausseneg, F. R. *Phys. Rev. Lett.* **2000**, *84*, 4721–4724. (b) Felidj, N.; Aubard, J.; Levi, G.; Krenn, J. R.; Hohenau, A.; Schider, G.; Leitner, A.; Aussenegg, F. R. *Appl. Phys. Lett.* **2003**, *82*, 3095–3097.
(29) Dick, L. A.; McFarland, D.; Haynes, L.; Van Duyne, R. P. *J. Phys. Chem. B* **2002**, *106*, 853–860.
(30) Haynes, C. L.; Van Duyne, R. P. *J. Phys. Chem. B* **2003**, *107*, 7426–7433.
(31) (a) Girlando, A.; Philpott, M. R.; Heitmann, D.; Swalen, J. D.; Santo, R. *J. Chem. Phys.* **1980**, *71*, 5187–5191. (b) Baltog, I.; Primeau, N.; Reinisch, R. *Appl. Phys. Lett.* **1995**, *66*, 1187–1189. (c) Kelf, T. A.; Sugawara, T.; Baumberg, J. J.; Abdelsalam, M.; Bartlett, P. N. *Phys. Rev. Lett.* **2005**, *95*, 1–4.

characterized previously.[35,36] The role of the overlap of the created chromophore with the laser excitation and the plasmon frequency can be tested by comparing the TTF⊂CBPQT^{4+} complex to one that generates a chromophore that does not have the spectral overlap. For this purpose, the 1:1 complex formed between CBPQT^{4+} and 1,5-dimethoxynaphthalene (DNP)[37] (Scheme 1b) gives rise to a CT transition ($\lambda_{max} = 530$ nm, $\epsilon = 800$ M^{-1} cm^{-1}, MeCN, 298 K). The importance of surface-adsorption is implicated from the surface selection rule and the vibrational band shifts of the SERS and SERRS data. Thus, (i) patterned and unpatterned substrates and (ii) color-matched and color-mismatched complexes are employed to verify that the wavelength-matching approach can be employed to achieve an active molecular plasmonics system.

Results and Discussion

Dependence of Plasmon Frequencies on Lattice Dimensions. The patterned substrates are based on gold-coated nanodisc arrays. The discs have diameters that are larger than those studied previously (50−200 nm).[26] Consequently, the plasmons were characterized using UV−vis−NIR reflectance spectroscopy and simulations, both conducted in air, to verify that these larger arrays retain tunable plasmons. The fabrication of the arrays is described in the Supporting Information. The lateral dimensions of the different gold nanodisc gratings were measured by scanning electron microscopy (SEM, Figure 2a), and the diameters, D, ranged from 600 to 1000 nm while the gaps, δ, ranged from 60 to 500 nm. The heights, h (75 nm), of the discs were determined by the thickness of gold that is necessary to ensure a continuous film is generated from disk to disk.

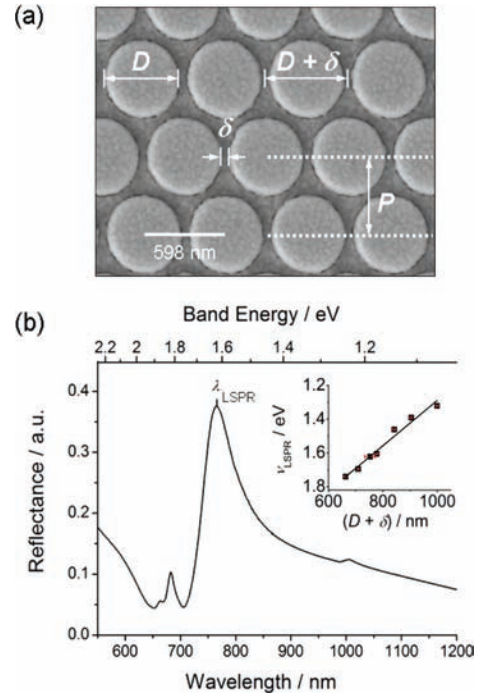

Figure 2. (a) SEM image of a typical nanodisc array with dimensions $D = 598$, $\delta = 65$, and $h = 75$ nm; P is the pitch and also corresponds to the first Bragg reflection (Supporting Information). (b) Reflectance spectrum of a gold nanodisc array ($D = 604$, $\delta = 150$ nm, air). Inset: ν_{LSPR} plotted against $(D + \delta)$ with a linear fit shown. The x-error bars are the standard deviations determined from SEM measurements.

The nanodisc arrays were patterned in 2 mm × 2 mm blocks separated by 0.1 mm of flat, unpatterned gold. Unpatterned gold-coated SiO_2/Si wafers were used as the reference background for reflectance measurements. The gratings exhibit (Figure 2b) a broad plasmon resonance (λ_{LSPR}) tailing to longer wavelengths as well as two weaker peaks at shorter wavelengths.[38] The energy position of the strongest plasmon, ν_{LSPR}, is linearly related (Figure 2b inset) to the lattice direction where the nanodiscs have their closest approach, $(D + \delta)$. The dependence of the energy position (ν_{LSPR}) of the most intense plasmon with $(D + \delta)$ suggests that the plasmons overlap[26] and localize between the discs upon irradiation with light normal to the surface. Thus, the interdisc region is predicted to contribute significantly to the SERS enhancements. Considering that the gaps span 65−400 nm, which is larger than most arrays,[26] it is encouraging to see enhancements of SERS spectra originating from the coupling between nanostructured metals can occur over similarly long distances, e.g., 120 nm.[39] The LSPR spectra were independent of polarization, which is consistent with the fact that, for hexagonal symmetry, the total contributions from the three lattice directions are independent of polarization angle.[26e]

The intensities of SERS spectra of *trans*-1,2-(4-pyridyl)ethylene (BPE) and self-assembled monolayers (SAMs) of 4-mercaptopyridine were characterized (Supporting Information) as a means for comparison to related substrates.[26] Enhancement factors of 10^8 were measured for BPE by a drop casting method.

(32) (a) Bozio, R.; Girlando, A.; Pecile, D. *Chem. Phys. Lett.* **1977**, *52*, 503–508. (b) Kuzmany, H.; Stolz, H. J. *J. Phys. C: Solid State Phys.* **1977**, *10*, 2241–2252. (c) Bozio, R.; Zanon, I.; Girlando, A.; Pecile, C. *J. Chem. Phys.* **1979**, *71*, 2282–2293. (d) Siedle, A. R.; Candela, G. A.; Finnegan, T. F.; Van Duyne, R. P.; Cape, T.; Kokoszka, G. F.; Woyciejes, P. M.; Hashmall, J. A. *Inorg. Chem.* **1981**, *20*, 2635–2640. (e) Bryce, M. R. *J. Mater. Chem.* **2000**, *10*, 589–598. (f) Segura, J. L.; Martín, N. *Angew. Chem., Int. Ed.* **2001**, *40*, 1372–1409. (g) Schukat, G.; Fanghänel, E. *Sulfur Rep.* **2003**, *24*, 1–282. (h) Becher, J.; Jeppesen, J. O.; Nielsen, K. *Synth. Met.* **2003**, *133*−*134*, 309–315. (i) Jeppesen, J. O.; Becher, J. *Eur. J. Org. Chem.* **2003**, 3245–3266. (j) *TTF Chemistry*; Yamada, J.-I., Sugimoto, T., Eds.; Kodansha: Tokyo, Japan, 2004. (k) See the special issue on Molecular Conductors: Batail, P. *Chem. Rev.* **2004**, *104*, 4887–5782. (l) Otsubo, T.; Takimiya, K. *Bull. Chem. Soc. Jpn.* **2004**, *77*, 43–58. (m) Canevet, D.; Salle, M.; Zhang, G.; Zhang, D.; Zhu, D. *Chem. Commun.* **2009**, 2245–2269.

(33) (a) Odell, B.; Reddington, M. V.; Slawin, A. M. Z.; Spencer, N.; Stoddart, J. F.; Williams, D. J. *Angew. Chem., Int. Ed. Engl.* **1988**, *27*, 1547–1550. (b) Anelli, P. L; et al. *J. Am. Chem. Soc.* **1992**, *114*, 193–218. (c) Asakawa, M.; Dehaen, W.; L'abbé, G.; Menzer, S.; Nouwen, J.; Raymo, F. M.; Stoddart, J. F.; Williams, D. J. *J. Org. Chem.* **1996**, *61*, 9591–9595.

(34) (a) Philp, D.; Slawin, A. M. Z.; Spencer, N.; Stoddart, J. F.; Williams, D. J. *J. Chem. Soc., Chem. Commun.* **1991**, 1584–1586. (b) Credi, A.; Montalti, M.; Balzani, V.; Langford, S. J.; Raymo, F. M.; Stoddart, J. F. *New J. Chem.* **1998**, *22*, 1061–1065.

(35) Witlicki, E. H.; Hansen, S. W.; Christensen, M.; Hansen, T. S.; Nygaard, S. D.; Jeppesen, J. O.; Jensen, L.; Wong, E. W.; Jensen, L.; Flood, A. H. *J. Phys. Chem. A* **2009**, *113*, 9450–9457.

(36) The resonance Raman spectrum also closely resembles the spectra of interlocked molecules constructed from the same TTF and CBPQT^{4+} components. (a) Nygaard, S.; Hansen, S. W.; Huffman, J. C.; Jensen, F.; Flood, A. H.; Jeppesen, J. O. *J. Am. Chem. Soc.* **2007**, *129*, 7354–7363. (b) For a SERRS spectrum of a surface-bound [2]rotaxane, see: Flood, A. H.; Wong, E. W.; Stoddart, J. F. *Chem. Phys.* **2006**, *324*, 280–290.

(37) Reddington, M. V.; Slawin, A. M. Z.; Spencer, N.; Stoddart, J. F.; Vicent, C.; Williams, D. J. *J. Chem. Soc., Chem. Commun.* **1991**, 630–634.

(38) Since λ_{LSPR} is the strongest plasmon and falls within the wavelength region of interest, it is the primary discussion point here. For assignments and discussion of the other plasmon modes, see the Supporting Information.

(39) Wei, W.; Li, S. Z.; Millstone, J. E.; Banholzer, M. J.; Chen, X. D.; Xu, X.; Schatz, G. C.; Mirkin, C. A. *Angew. Chem., Int. Ed.* **2009**, *48*, 4210–4212.

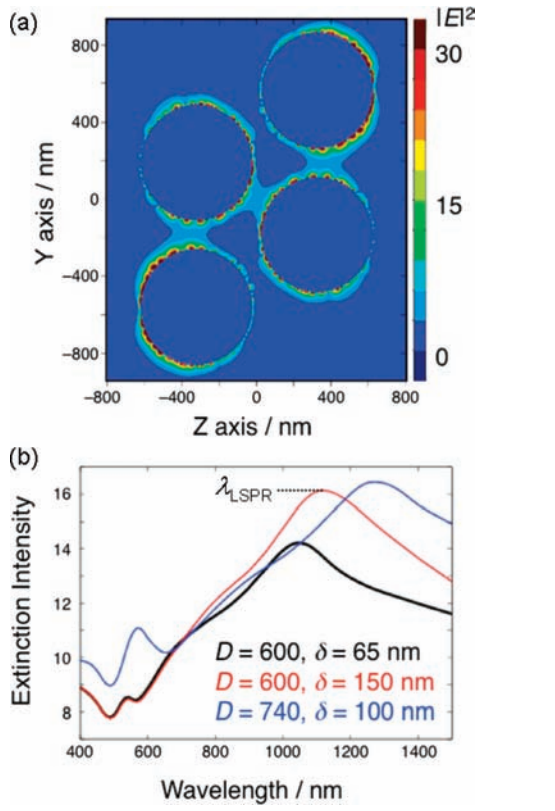

Figure 3. (a) The electric field distribution ($|E|^2$) calculated for a gold nanodisc tetramer with dimensions used in the SERRS experiments (D = 600 and δ = 150 nm) at a wavelength resonant with λ_{LSPR}. The polarization is along the *y*-axis and shows a maximum $|E|^2$ value of 300. The intensity scale is limited to 30 to better visualize the interdisc region. (b) Simulated extinction spectra for gold nanodisc trimers with three different dimensions in air.

For SAMs of 4-mercaptopyridine, the intensity enhancements scale, as expected, with the D/δ ratio.[26e]

To understand further the plasmonic properties of the nanodisc array, the extinction spectra of monomers, dimers, trimers, and tetramers (Figure 3a) of the gold nanodiscs were simulated using the discrete dipole approximation (DDA, Supporting Information).[40] There have been several simulations of the extinction properties of 2D arrays of gold nanodiscs;[26,27] however, the diameters of the discs in this work (593−824 nm) are approximately an order of magnitude larger than most previous works (50−200 nm). The simulated extinction spectra for a gold nanodisc trimer with dimensions corresponding to the experimental spectra (Supporting Information) are shown in Figure 3b. The extinction spectra show a strong peak around 1100−1300 nm and a weaker peak around 550 nm. The strong peak is characterized as an in-plane dipole plasmon resonance (see Figure 3a for the electric field distribution of the tetramer's intense LSPR) and is found to blue-shift significantly when (D + δ) is decreased and when the number of discs is increased; i.e., for an isolated particle this peak is found around 1500 nm (Supporting Information). Therefore, this peak is assigned to λ_{LSPR}, which is found experimentally between 700 and 850 nm. A larger number of discs would account for the difference between experiment (~8 × 10^6 discs in each 2 × 2 mm^2 patterned region) and theory.

(40) Draine, B. T.; Flatau, P. J. *J. Opt. Soc. Am. A* **1994**, *11*, 1491–1499.

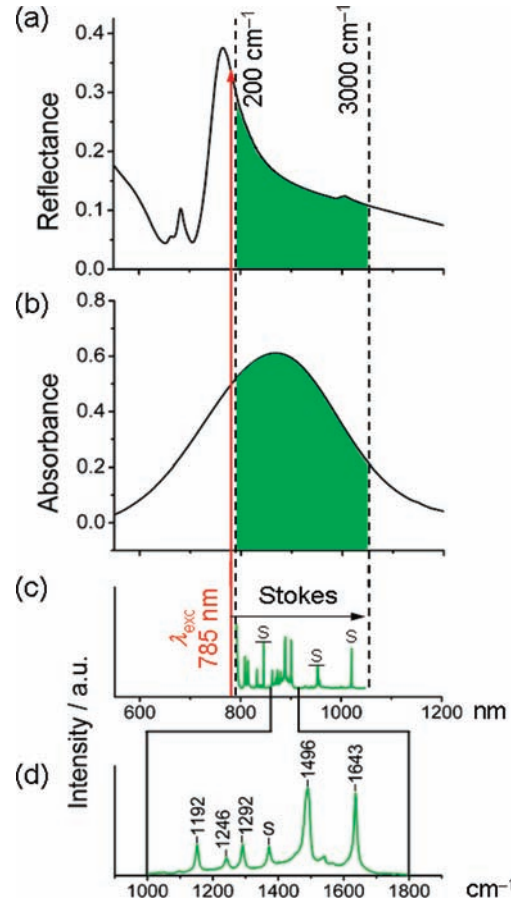

Figure 4. Representation of the wavelength-matching approach: (a) UV−vis−NIR reflectance spectrum of a gold-coated nanodisc array in air, (b) a UV−vis−NIR spectrum of TTF⊂$CBPQT^{4+}$ in MeCN, (c) the absolute wavelength resonance-Raman scattering spectrum of TTF⊂$CBPQT^{4+}$ in MeCN and (d) detail of the Raman-shifted chromophore-specific vibrations (in cm^{-1}). Solvent bands are marked as S. Conditions: (a) D = 604, δ = 150, and h = 75 nm; (b) 0.2 mM $CBPQT^{4+}$ + 2 mM TTF, MeCN; (c and d) 17 mM $CBPQT^{4+}$ + 17 mM TTF, λ_{exc} = 785 nm, 30 mW, average of five 60 s accumulations, MeCN.

Surface Enhancement of the Resonance Raman Scattering Spectrum. On the basis of the plasmon tuning, a nanoarray with parameters D = 604 nm and δ = 150 nm (Figures 2b, 3b, red trace and 4a) is hypothesized to be wavelength matched with the CT chromophore of the TTF⊂$CBPQT^{4+}$ complex to generate surface-enhanced spectra. The intense plasmon resonance (λ_{LSPR} = 765 nm, Figure 4a) lies on the blue side of the λ_{max} (865 nm) of the CT chromophore (Figure 4b). The relation between Raman scattering intensity, I, and the local electric field strength, E, is usually approximated as $I \propto |E|^4$.[13] The DDA simulations show that the $|E|^2$ can reach values of ~300 for these dimensions which indicate SERS enhancements on the order of $I \propto |E|^4 \approx 10^4-10^5$. This intensity relation can also be separated as[13d,26e,41] $I_{SERS} \propto |E(\lambda_{exc})|^2 \cdot |E(\text{Raman})|^2$, where $E(\lambda_{exc})$ and E(Raman) are the electric field strengths and associated enhancements[13d,42] at the laser excitation and Stokes-shifted Raman scattered energies, respectively. Therefore, with both the LSPR and supramolecular chromophore extending across the wavelength range covered by the Stokes scattered light (Figure 4c), multiple sources of SERRS signal enhance-

(41) Zeman, E. J.; Schatz, G. C. *J. Phys. Chem.* **1987**, *3*, 634–643.
(42) McFarland, A. D.; Young, M. A.; Dieringer, J. A.; Van Duyne, R. P. *J. Phys. Chem. B* **2005**, *109*, 11279–11285.

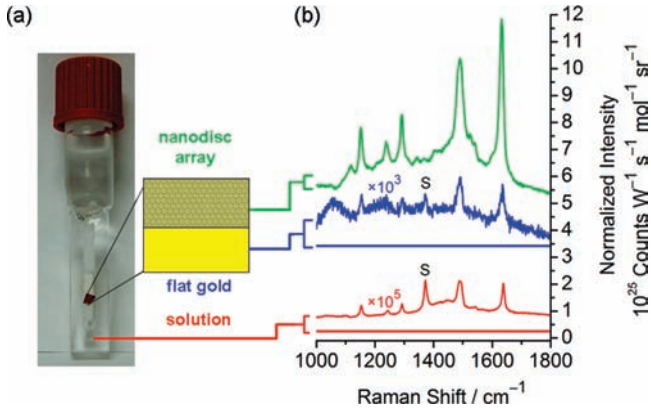

Figure 5. (a) Apparatus setup for creating thin film solutions (path length <1 μm) over the nanodisc arrays. (b) Normalized Raman spectra (λ_{exc} = 785 nm) of the TTF⊂CBPQT^{4+} complex (1 mM CBPQT^{4+} + 3 mM TTF, MeCN, 298 K) from the array (top green trace), flat gold (middle blue traces), and solution (bottom red traces). Solvent bands are labeled as S.

ment are provided. For 785 nm excitation, the wavelength range corresponding to 0−1700 cm^{-1} (Figure 4d) covers 785−906 nm. Lastly, this choice of lattice parameters is a balance between maximizing the spectral overlap of the various components and optimizing the diameter spacing ratio,[26e] D/δ, for higher enhancement factors.

Chromophore−plasmon coupling was verified when the observed resonance Raman scattering spectra (Figure 5) were assigned to originate from the SERRS effect. The array (Figure 5a) was placed in contact with a thin layer (<1 μm) of a solution of the complex with ∼90% complexation (MeCN, 1 mM CBPQT^{4+} + 3 mM TTF, 298 K) inside a wafer−cartridge assembly (Supporting Information), and the patterned gold surface was irradiated through the solution[22b] with a resonant wavelength (λ_{exc} = 785 nm).[43] An intense spectrum[35] (Figure 5b, green trace) is observed from the patterned gold surface. Compared to the solution-based resonance Raman spectrum, each of the intense bands is surface enhanced by a factor of ∼3 × 10^5 (*vide infra*). This value is consistent with that observed from the drop-cast BPE sample (×10^8).[44] The surface spectrum's similarity to solution indicates that the complex's chromophore has been generated. Such a similarity between solution and surface spectra recorded under resonance conditions was also observed with rhodamine-6G.[45] By marked contrast, the resonance Raman spectrum is only weakly enhanced from the flat gold region (Figure 5b, blue trace). The resonance Raman scattering bands originating from solution (Figure 5b, red trace) are weaker still. These data indicate that the resonance Raman spectrum from the complex in the patterned region is surface-enhanced; i.e., a SERRS spectrum is generated. Enhancement of the vibrational bands is mainly attributed to the wavelength overlap (Figure 4) between the CT transition of the complex (λ_{max} = 865 nm), the laser excitation (λ_{exc} = 785 nm), and the surface plasmon (λ_{LSPR} = 765 nm).

(43) Using the wafer-cartridge assembly (Supporting Information), spot-to-spot reproducibility was estimated to be 20% and the MeCN bands at 919, 1375, and 2254 cm^{-1} serve as reliable internal intensity standards. See Supporting Information for more details.

(44) The EF calculated using eq S1 in the Supporting Information is principally based on an estimate of the different scattering volumes in solution for resonance Raman and at the surface of the nanodiscs for the SERRS while using solvents as intensity standards; see Supporting Information for more details.

(45) (a) Jensen, L.; Schatz, G. C. *J. Phys. Chem. A* **2006**, *110*, 5973–5977. (b) Shim, S.; Stuart, C. M.; Mathies, R. A. *ChemPhysChem* **2008**, *9*, 697–699.

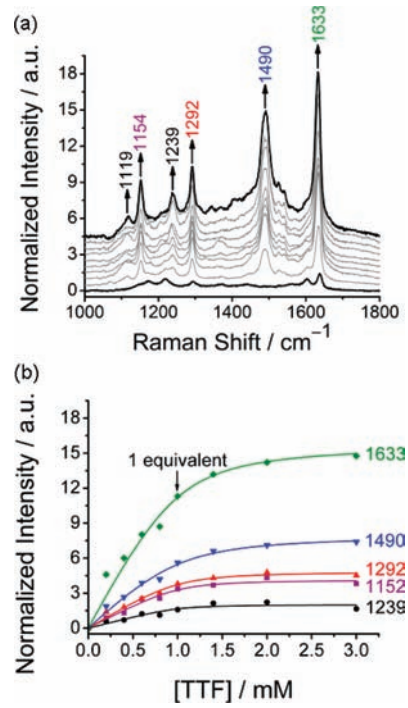

Figure 6. Titration of TTF into 1 mM CBPQT^{4+} (up to 3 mM TTF, MeCN, 298 K, λ_{exc} = 785 nm) observed using (a) SERRS (spectra offset) with (b) titration curves fit to a 1:1 model.

"Turning On" Resonant SERRS by Formation of the TTF⊂CBPQT^{4+} Complex. To confirm that the resonance effect must act in concert with the plasmonic field to account for the large intensities, a titration of the TTF guest into the CBPQT^{4+} was conducted. Such an experiment also serves as a means to confirm the quantitative character of this SERS/SERRS platform.[8d] Initially, the spectrum from the solution of the empty CBPQT^{4+} host (1 mM, MeCN) is assigned to normal SERS scattering. Interpretations of this spectrum are outlined in the next section. The TTF was titrated (Figure 6a) as a solid using a tip-drying method[35] to keep the concentration of CBPQT^{4+} constant. During the additions of TTF, resonantly enhanced CBPQT^{4+}-based vibrational bands grow in concomitantly at 1633, 1292, 1239, and 1154 cm^{-1} along with the TTF-based band at 1490 cm^{-1} (Figure 6a). These bands were previously assigned to the subunits of the complex on the basis of the similarity to the computed spectrum obtained under resonance Raman conditions.[35] The extra enhancement of the intensity of the vibrational spectrum and the transformation from the SERS of CBPQT^{4+} into the spectrum of the complex confirms the importance of the resonance contribution to the SERRS spectrum.

The extent to which each band is enhanced by resonance is vibration-dependent. The enhancement factors that can be calculated from the spectra before and after addition of the TTF guest are phenomenological in character. This situation emerges because the specific form of the normal modes of vibration of the CBPQT^{4+} host can change[35] to a smaller or larger degree upon TTF guest binding. Therefore, the extent to which the spectrum is "turned on" in Figure 6a is similar in character to the spectral enhancements seen with fluorescence sensing. The 1633, 1292, and 1154 cm^{-1} SERRS bands of CBPQT^{4+}, which have corresponding SERS bands at 1638, 1294, and 1173 cm^{-1}, show turn-on factors of ×10, ×4 and ×3, respectively. It is interesting to note that the spectral enhancement factors for these

bands as measured in solution are ×31, ×12, and ×26. By contrast, the SERRS bands at 1239 and 1119 cm^{-1} are not even observed in the SERS spectrum of the empty $CBPQT^{4+}$ host (Figure 6a) such that the turn-on factors cannot be quantified. Furthermore, the fact that the SERS spectrum of TTF can only be observed under special conditions[46] indicates that the 1490 cm^{-1} band of TTF as well as the 1239 and 1119 cm^{-1} bands all enjoy a huge turn-on effect from a "zero" starting point. The appearance of the TTF band indicates that resonance acts together with preconcentration of TTF at the surface (by complexation with the $CBPQT^{4+}$ host) to enhance the intensity of this vibration.

Fitting the SERRS band intensities from the titration data to binding curves (Figure 6b) using a standard 1:1 model[47] generates an average binding constant of $K_a = 14\,000\ M^{-1}$ corresponding to a binding energy of $\Delta G = -5.6 \pm 0.3$ kcal mol^{-1} at 298 K. This value agrees with the binding strengths of this complex established from prior results measured using several different methods (Supporting Information).[35,48−50] The deviations to the fit in the intensity of the 1633 cm^{-1} band at 0.2 equiv can be attributed to the SERS intensity from $CBPQT^{4+}$ present at the beginning of the titration.

Surface Adsorption of the $CBPQT^{4+}$ Host and Its Complexes. While the wavelength-matching (Figure 4) that occurs upon TTF binding is shown to be important for resonance enhancement and the plasmons from the patterned region are required for surface enhancement, surface adsorption is also relevant to the SERS effect. Here, we examine and identify the importance of the surface-adsorbed host for bringing all the species close to the surface. The SERS and SERRS data highlight shifts in vibrational band positions and changes in the intensity pattern that are indicative[5g] of surface adsorption.

The solution and SERS spectrum of $CBPQT^{4+}$ (Figure 7a and b, respectively) have different intensity *patterns*. This difference indicates that there is an order-induced change in the relative band intensities, stemming from the surface-selection rule,[13,51] which must arise from surface adsorption. The ordering of $CBPQT^{4+}$ at surfaces (air−water interface,[52] graphite[53]) has been observed previously. In such cases, the close approach of the empty tetracationic cyclophanes, as seen in the crystal structure of $CBPQT{\bullet}4PF_6{\bullet}3MeCN$,[33a] is believed to be mediated by the four hexafluorophosphate (PF_6^-) anions. The most notable intensity differences are the large increases in the phenylene-based[54] vibrational band upon moving from solution (1618 cm^{-1}) to the surface (1602 cm^{-1}) and the emergence of the vibrational band at 1219 cm^{-1}. The latter observation has been seen previously in the SERS spectra recorded from a roughened Ag electrode[3a] of the paraquat dication, which are subunits of the $CBPQT^{4+}$ host. Consistent with surface adsorption, there is a shifting in the position of some of the $CBPQT^{4+}$ bands (Table 1) compared to solution.[35] For example, the 1650 cm^{-1} band shifts 12 cm^{-1} to lower energy in the SERS spectrum. These shifts are consistent with previous observations of surface adsorption.[55]

By contrast to $CBPQT^{4+}$, the TTF showed no SERS response, either by comparison to bands seen from the solid state (Supporting Information)[35,56] or for solution, even up to a concentration of 200 mM (CH_2Cl_2). The SERS spectra of TTF have only been observed once before[55] and only by pretreating some silver powder with excess sodium borohydride. Thus, under our conditions, there is no surface adsorption.

For the TTF⊂$CBPQT^{4+}$ complex, the similarity between the SERRS spectra (Figure 7c) and the solution-phase resonance

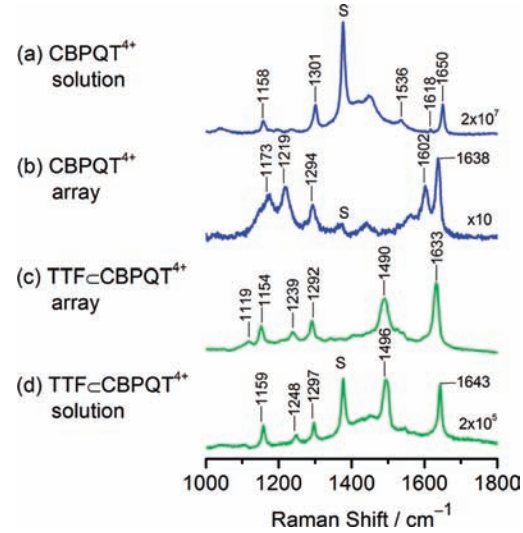

Figure 7. Comparisons of the surface and solution Raman spectra (λ_{exc} = 785 nm, 30 mW, MeCN, 298 K) of (a,b) empty $CBPQT^{4+}$ host and (c,d) the TTF⊂$CBPQT^{4+}$ complex in complementary conditions. Solvent bands are labeled as S. Conditions: (a) 1 mM $CBPQT^{4+}$ + 3 mM TTF, 1 acquisition, 10 s; (b) 1 mM $CBPQT^{4+}$ + 3 mM TTF, average of 10 × 10 s acquisitions; (c) 1 mM $CBPQT^{4+}$, one 10 s acquisition; (d) 30 mM $CBPQT^{4+}$, average of 5 × 60 s acquisitions.

Table 1. Selected Band Positions, Intensities, Full Width at Half Maximum (FWHM) Values (in Parentheses), and Enhancement Factors (EF) of the Unbound $CBPQT^{4+}$ Receptor in the Region above 1000 cm^{-1} Both in Solution and Interfaced with the Nanodisc Arrays[a]

ν_{NRS}[b] (cm^{-1})	I_{NRS}[c]	ν_{SERS}[d] (cm^{-1})	I_{SERS}[c]	$\Delta\nu$	EF
1650 (8)	1.2×10^{17}	1638 (13)	2.4×10^{23}	−12 (+5)	2×10^6
1618 (3)	3.0×10^{15}	1602 (15)	1.8×10^{23}	−16 (+12)	6×10^7
1536	2.5×10^{16}			−	−
1301 (11)	9.0×10^{16}	1294 (15)	1.7×10^{23}	−7 (+4)	2×10^6
		1219	2.1×10^{23}	−	−
		1173	1.9×10^{23}	−	−
1158	5.4×10^{16}			−	−

[a] Corresponding spectra are found in Figure 7a and 7b. [b] Solution phase (MeCN). NRS = normal Raman scattering. [c] Units are counts W^{-1} s^{-1} mol^{-1} sr^{-1}. [d] Thin film of solution (~1 μm, MeCN) over nanodisc arrays (D = 604, δ = 150 nm).

(46) Nie, S.; Yu, N.-T. *J. Raman Spectrosc.* **1991**, *22*, 489–495.
(47) Long, J. R.; Drago, R. S. *J. Chem. Educ.* **1982**, *59*, 1037–1039.
(48) Ashton, P. R.; Balzani, V.; Becher, J.; Credi, A.; Fyfe, M. C. T.; Mattersteig, G.; Menzer, S.; Nielsen, M. B.; Raymo, F. M.; Stoddart, J. F.; Venturi, M.; Williams, D. J. *J. Am. Chem. Soc.* **1999**, *121*, 3951–3957.
(49) Ashton, P. R; et al. *Chem.−Eur. J.* **1997**, *3*, 152–170.
(50) Choi, J. W.; Flood, A. H.; Steuerman, D. W.; Nygaard, S.; Braunschweig, A. B.; Moonen, N. N. P.; Laursen, B. W.; Luo, Y.; DeIonno, E.; Peters, A. J.; Jeppesen, J. O.; Xu, K.; Stoddart, J. F.; Heath, J. R. *Chem.−Eur. J.* **2006**, *12*, 261–279.
(51) (a) Moskovits, M. *J. Chem. Phys.* **1982**, *77*, 4408–4416. (b) Moskovits, M.; Suh, J. S. *J. Phys. Chem.* **1984**, *88*, 5526–5530.
(52) Ahuja, R. C.; Caruso, P.-L.; Mobius, D.; Wildburg, G.; Ringsdorf, H.; Philp, D.; Preece, J. A.; Stoddart, J. F. *Langmuir* **1993**, *9*, 1534–1544.
(53) Laitenberger, P.; Claessens, C. G.; Kuipers, L.; Raymo, F. M.; Palmer, R. E.; Stoddart, J. F. *Chem. Phys. Lett.* **1997**, *279*, 209–214.
(54) For vibrational band assignment, please see Supporting Information in ref 35.
(55) Lu, T.; Cotton, T. M. *J. Phys. Chem.* **1987**, *91*, 5978–5985.
(56) (a) Sandroff, C. J.; Weltz, D. A.; Chung, J. C.; Herschbach, D. R. *J. Phys. Chem.* **1983**, *87*, 2127–2133. (b) Joy, V. T.; Srinivasan, T. K. K. *Chem. Phys. Lett.* **2000**, *328*, 221–226.

Table 2. Selected Spectroscopic Data of the TTF⊂CBPQT^{4+} Complex in the Region above 1000 cm^{-1} Both in Solution and Interfaced with the Nanodisc Arrays[a]

ν_{RRS}[b] (cm^{-1})	I_{RRS}[c]	ν_{SERRS}[d] (cm^{-1})	I_{SERRS}[c]	$\Delta\nu$	EF
1643 (10)	6×10^{18}	1633 (15)	2×10^{24}	−10 (+5)	2×10^{5}
1496 (20)	6×10^{18}	1490 (26)	1×10^{24}	−6 (+6)	2×10^{5}
1297 (8)	2×10^{18}	1292 (11)	7×10^{23}	−5 (+3)	4×10^{5}
1248 (9)	9×10^{17}	1239 (15)	5×10^{23}	−9 (+6)	5×10^{5}
1159 (9)	2×10^{18}	1154 (14)	6×10^{23}	−2 (+5)	3×10^{5}

[a] Corresponding spectra are found in Figure 8c and 8d. FWHM in parentheses. [b] Solution phase (MeCN). [c] Units are counts W^{-1} s^{-1} mol^{-1} sr^{-1}. [d] Thin film of solution (~1 μm, MeCN) over nanodisc arrays (D = 604, δ = 150 nm).

Raman scattering (Figure 7d) indicates that the mechanisms of enhancement that control the relative intensity *pattern* stem more from chromophore−plasmon coupling than from the surface selection rule.[45] Nevertheless, there exists evidence for the complex's adsorption to the surface. The fact that both the TTF- and CBPQT^{4+}-based bands of the complex all shift to lower energies in the SERRS spectrum (Table 2) is consistent with the retention of the surface interaction seen for the empty CBPQT^{4+} host. While there is no strong evidence[57] that the complex is ordered on the surface, ordering of the complexes is common to other systems. For instance, the crystal structure of the TTF⊂CBPQT•4PF$_6$ complex[34a] shows a similar anion-mediated ordering as the parent host system CBPQT•4PF$_6$•3MeCN structure.[33a] Computational[58] and experimental[59] results on surface-confined, bistable rotaxanes incorporating both the TTF and DNP subunits (Scheme 1b) show that it is the CBPQT^{4+} ring that dictates the surface packing.

Consistent with surface adsorption of the complex is the fact that the binding constants obtained from SERRS and the solution-phase techniques (Supporting Information) are similar. They can only be similar if the surface affinity of both CBPQT^{4+} and TTF⊂CBPQT^{4+} are also similar. Regarding the sequence of events leading to binding, since the TTF is delivered to solution far from the surface, it is reasonable to assume that it arrives at the surface already complexed. The complex can either adsorb to the surface by displacing the empty CBPQT^{4+} or by dynamic equilibration of the TTF unit with the surface-adsorbed CBPQT^{4+} host. The similar surface affinities of CBPQT^{4+} and the TTF⊂CBPQT^{4+} complex facilitate the wavelength-matching approach: surface adsorption localizes the chromophore at the surface where the plasmon's electric field is at its most intense. Thus, surface adsorption is also an essential part of the "turn-on" effect.

Control Study with a Nonresonant Complex. To investigate some of these ideas further, a control experiment was conducted in which DNP (Scheme 1b) was utilized as a guest for CBPQT^{4+}. The resulting CT complex, DNP⊂CBPQT^{4+},[34a,37] closely resembles the one formed with TTF. However, it differs from the TTF⊂CBPQT^{4+} complex in one key way: Its CT chromophore absorbs in the middle of the visible region (Figure 8a, λ_{max} = 530 nm, ε = 800 cm^{-1} M^{-1}, MeCN, 298 K).[60] This property difference allows for the creation of a CT chromophore at the solution−surface interface that is resonant with neither the plasmon (λ_{LSPR} = 765 nm) nor the excitation laser (λ_{exc} = 785 nm). Under these conditions, any enhancement from the DNP⊂CBPQT^{4+} complex should have no contribution from chromophore-plasmon coupling. If the proposed mechanism of enhancement is correct, the DNP⊂CBPQT^{4+} complex should have a similar surface affinity as TTF⊂CBPQT^{4+} [61] and achieve

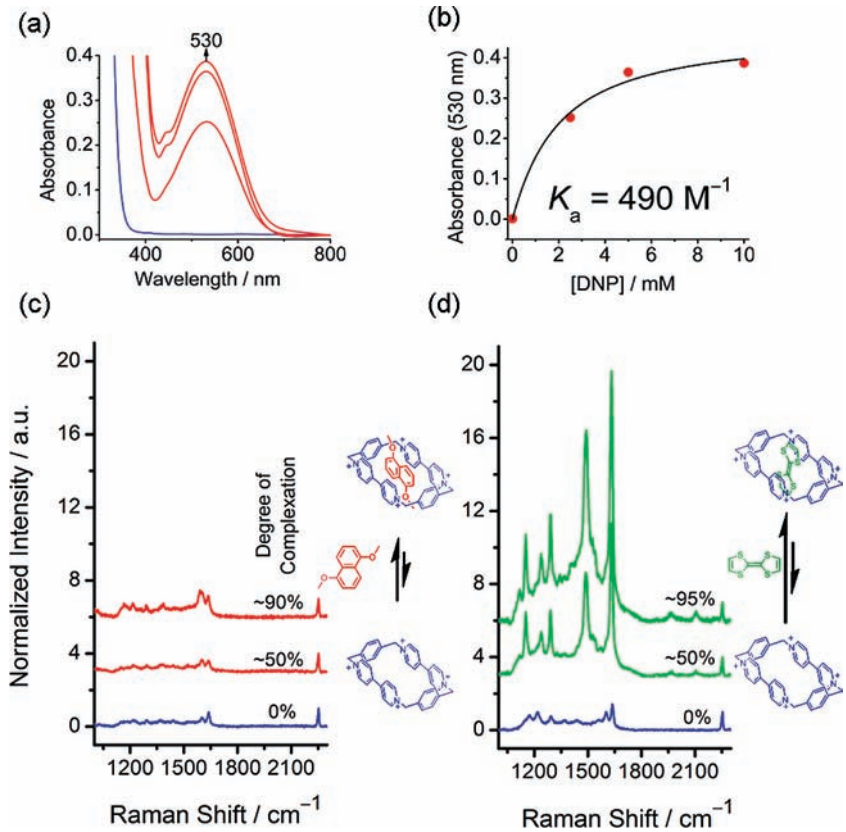

Figure 8. (a) UV−vis−NIR titration of DNP into CBPQT^{4+} (1 mM, MeCN, 298 K) and (b) its corresponding binding curve. Raman spectra (λ_{exc} = 785 nm) of CBPQT^{4+} (SERS, bottom blue traces), (c) DNP⊂CBPQT^{4+} (SERS, red traces), and (d) TTF⊂CBPQT^{4+} (SERRS, green traces) at different degrees of complexation (0, ~50, and >90% from bottom to top).

a SERS spectrum from the plasmonic field it encounters when it is located at the surface of the patterned gold.

The nonresonant SERS spectra of DNP⊂CBPQT^{4+} (Figure 8c) generated by titration with the DNP guest show markedly weaker intensities than the SERRS spectra (Figure 8d) of the TTF⊂CBPQT^{4+} complex. Moreover, the intensities barely differ from those of the surface-ordered CBPQT^{4+} host alone.[61] Formation of the DNP⊂CBPQT^{4+} complex is confirmed by the small shift (-2 cm^{-1}) in the 1638 cm^{-1} band and the emergence of a band at 1582 cm^{-1}, which is diagnostic of the DNP⊂CBPQT^{4+} complex (Supporting Information). The fact that the main difference between the two complexes is the absorption wavelength of the CT chromophores, once again, indicates that spectral overlap between chromophore, plasmon, and excitation wavelength is a determining factor leading to the observed enhancement in the SERRS spectra of the TTF⊂CBPQT^{4+}.

Conclusions

Creating a chromophore upon complexation between TTF guest and CBPQT^{4+} host turns on the intensity of a SERRS spectrum. The presence of the plasmon and of the chromophore are necessary for achieving the observed turn-on effect. Surface adsorption by the CBPQT^{4+} host when it is empty or complexed is critical for situating the supramolecular chromophore at the surface where the plasmons are most intense. The creation of a plasmonic device that responds to the addition of the guest molecule and the subsequent coupling of the CT chromophore to the LSPR both aid in unifying elements of supramolecular chemistry with active molecular plasmonics.

Experimental Section

General Methods. Acetonitrile (MeCN) (Mallinckrodt, R&D grade) was distilled over CaH_2 (Aldrich, 95%) and degassed with Ar (Airgas, ultrahigh purity). Tetrathiafulvalene (TTF) (Fluka, HPLC grade) was used without purification. The cyclophane cyclobis(paraquat-*p*-phenylene) (CBPQT^{4+}), which was used as the tetrakis(hexafluorophosphate) salt, was prepared using standard methods.[33] The 1,5-dimethoxynaphthalene (DNP) was synthesized according to literature procedures.[62]

Raman Spectroscopy. Raman data were recorded using a Renishaw inVia Raman microscope fitted with a diode laser (Renishaw) for 785 nm excitation. The instrument was interfaced with a light microscope (Leica) fitted with a 50× long working distance objective (Leica; numerical aperture 0.5) generating a 22 μm × 3 μm spot or a 50× short working distance objective (Leica; numerical aperture 0.75) with a 28 μm × 3 μm spot. For solution-phase Raman and the SERRS experiments, a 90° mirror attachment and cell holder (Renishaw) were used. The spectrometer was wavelength-calibrated using Si (520.5 cm^{-1}). Laser powers used in the experiments were adjusted to ensure sample integrity for the duration of each experiment, usually 3 mW. The MeCN solvent band at 2254 cm^{-1} was used as an internal intensity standard. No corrections for spectrometer sensitivity or self-absorption were conducted. The Raman spectroscopy used to determine the SERS performance of arrays with BPE and 4-mercaptopyridine was done using a Kaiser HoloLab5000. The Raman spectra were obtained at 633 and 785 nm using a 50× objective with a numerical aperture of 0.75. Spectra were baselined when appropriate.

UV−vis−NIR Spectroscopy. Electronic absorption spectra were recorded using a Cary 5000 UV−vis−NIR spectrometer. The reflectance spectra from nanodisc gratings were obtained at normal incidence reflectance by fitting the spectrometer with a 50:50 polka dot beam splitter. For solution phase spectroscopy, quartz cuvets were purchased from Starna Cells, Inc. UV−vis−NIR spectra were recorded from 200−1200 at 600 nm min^{-1}.

Substrate Characterization. The dimensions of the substrates were characterized by scanning electron microscopy (SEM) using a JEOL 6700, by profilometry using a Dektak 8, and by atomic force microscopy (AFM) using a DI Dimension 5000.

Acknowledgment. Indiana University (A.H.F.); the Strategic Research Council in Denmark (Project #2117-05-0115), and the Villum Kann Rasmussen Foundation for financial support (J.O.J.); and The Pennsylvania State University for funds and the Research Computing and Cyberinfrastructure (L.J.); and National Aeronautics and Space Administration (NASA) for funds (E.W.W.).

Supporting Information Available: Procedures for the preparation and characterization of the nanodisc arrays, the construction of the wafer cartridge assembly, quantifying SERS and SERRS enhancement factors, dimension tunability of the plasmons, experimental procedures for spot-to-spot reproducibility and signal vs focus of the arrays, experimental details for the titrations of CBPQT^{4+} with TTF and DNP, thermodynamic analysis, expanded plots of SERRS titration spectra, details for electrodynamics simulations, and complete refs 33b and 49. This material is available free of charge via the Internet at http://pubs.acs.org.

JA910155B

(57) The only evidence for the surface selection rule, and thus molecular ordering, arises from the observation of the 1119 cm^{-1} band. While this band is weakly enhanced in the SERRS spectrum, it is not even observed in the solution resonance Raman spectrum (Figure 7d).

(58) (a) Jang, S. S.; Jang, Y. H.; Kim, Y.-H.; Goddard, W. A.; Flood, A. H.; Laursen, B. W.; Tseng, H.-R.; Stoddart, J. F.; Jeppesen, J. O.; Choi, J. W.; Steuerman, D. W.; DeIonno, E.; Heath, J. R. *J. Am. Chem. Soc.* **2005**, *127*, 1563–1575. (b) Jang, S. S.; Jang, Y. H.; Kim, Y.-H.; Goddard, W. A.; Choi, J. W.; Heath, J. R.; Laursen, B. W.; Flood, A. H.; Stoddart, J. F.; Norgaard, K.; Bjornholm, T. *J. Am. Chem. Soc.* **2005**, *127*, 14804–14816.

(59) Nørgaard, K.; Laursen, B. W.; Nygaard, S.; Kjaer, K.; Tseng, H.-R.; Flood, A. H.; Stoddart, J. F.; Bjørnholm, T. *Angew. Chem., Int. Ed.* **2005**, *44*, 7035–7039.

(60) The binding strength with CBPQT^{4+} is approximately 10 times smaller than that with TTF (K_a = 490 M^{-1}, MeCN, 298 K), which merely dictates that, for this titration, more molar equivalents of DNP were used to achieve the same level of complexation for comparative purposes.

(61) The solid-state structure of the DNP⊂CBPQT•4PF_6 complex (see ref 37) is essentially isostructural with that of CBPQT•4PF_6•3MeCN (see ref 33a), suggesting they will have similar surface affinities.

(62) Dotz, K. H.; Popall, M. *Chem. Ber.* **1988**, *121*, 665–672.